Synthesis, Phase Behaviors, and Mechanical Properties of Biphenyl-Type Epoxy Resins and Composites

Shaoping Ren,[1–3] Liyan Liang,[1–3] Yanxun Lan,[2] Mangeng Lu[1,2]

[1]Guangdong Key Laboratory of Polymer Materials for Electronics, Guangzhou 510650, People's Republic of China
[2]Guangzhou Institute of Chemistry Chinese Academy of Sciences, Guangzhou 510650, People's Republic of China
[3]Graduate School of the Chinese Academy of Science, Beijing 100039, People's Republic of China

ABSTRACT: Diglycidyl ether of 3,3′,5,5′-tetramethyl-4,4′-biphenyl (TMBPDGE) which has been found great applications in semiconductor packaging was synthesized. The liquid crystalline phases of diglycidyl ether of 4,4′-dihydroxybiphenol (BPDGE) cured with phenol novolac (PN) were studied by wide angle X-ray diffraction (WAXD) and polarized optical microscopy (POM). BPDGE was *in situ* copolymerized with TMBPDGE to improve its thermal and mechanical properties by means of the LC domains retained in the crosslinked networks. The results indicated that a nematic phase was formed and fixed with proper curing schedule when BPDGE was cured with PN that had no neighboring active hydrogens and the LC domains could also be efficiently embedded into the composite systems. Dynamic mechanical properties showed that epoxy networks containing LC domains displayed higher α-relaxation temperature and linear elastic modulus traces. The impact toughness and T_g were improved with the addition of BPDGE. Scanning electron microscope observation of the fracture surfaces showed that there was a change in failure mechanism in the composite systems. © 2007 Wiley Periodicals, Inc. J Appl Polym Sci 106: 2917–2924, 2007

Key words: epoxy; liquid-crystalline polymers (LCP); polymer composites; toughness

INTRODUCTION

Epoxy resins are used in a wide variety of applications ranging from structural composites to microelectronics thanks to its good heat resistance, moisture resistance, electrical properties, and excellent adhesiveness. However, the structure of epoxy resins, of thermosets in general, leads to low toughness, and this drawback results in its low reliability when using in electronic component encapsulations. A significant amount of academic research, therefore, has been devoted to solving this problem.

One of the most developed approaches is obtaining a dispersion consisting of a particulate second phase such as reactive rubbers or thermoplastics in the thermosetting polymer. Particularly, when using reactive liquid rubber to tough thermosets, although the toughness of epoxy resins is improved; however, their T_g, modulus and mechanical properties are decreased consequently because of the copolymerized systems undergo a phase separation during curing.[1–4] Thermoplastics can avoid such problems, but its high viscosity also leads to the blends difficult processing.[5–9]

Liquid crystalline epoxy resins (LCERs) were first patented in the late 1980[10,11] and they were intensively investigated for last one decade. Many research groups reported the synthesis, curing behavior, phase transition, thermal properties, bonding properties, and mechanical and electrical characteristics of various LCE resins.[12–17] They also investigated the mechanical properties of LCERs when cured in magnetic or electrolic fields.[18–21] As compared to ordinary epoxies, after cured, LCERs exhibit higher toughness due to the crack propagation is retarded by the formation of many LC domains in the curing networks.[22–24] Therefore, LCERs can be a potential candidate for composite application to obtain resins with high T_g, high modulus and superior fracture toughness.[25,26]

Diglycidyl ether of 3,3′,5,5′-tetramethyl-4,4′-biphenyl(TMBPDGE) is a commercial epoxy which can be widely applied as encapsulation material because of the good adhesion, low viscosity, and high filler loading.[27] Diglycidyl ether of 4,4′-dihydroxybiphenol (BPDGE) shows liquid crystal phase while cured with aromatic amine as reported in previous studies.[28–31] In our previous works, the curing, phase change, thermal, and mechanical properties of BPDGE were studied.[32,33] Farren et al.[23] reported that BPDGE had higher temperature α-relaxations, more linear elastic modulus traces and lower water absorption than TMBPDGE. Ochi et al. investigated the optical and thermal and mechanical properties of BPDGE with different phenolic curing agents. They concluded that when phenol novolac (PN) was used to cure BPDGE, the active hydrogens were distributed in a random

WILEY
InterScience®
DISCOVER SOMETHING GREAT

direction. As a result, the biphenol groups in the epoxy molecules could not form LC domains in the networks.[28,34]

In this study, however, it was found that when BPDGE/PN was cured at a relative low temperature, LC monomers formed a nematic phase before extensive crosslinking took place. This means that BPDGE/ PN can also form a microdomain ordered structure despite PN has no neighboring active hydrogens. In addition, BPDGE was selected to *in situ* copolymerized with TMBPDGE to improve its thermal and impact toughness. Dynamic Themomechanical Analyzer (DMA) was conducted to investigate the micro mechanical properties of various kinds of networks. We also discussed the effects of an addition BPDGE on the glass transition temperature of the composites and investigated the fracture behavior of liquid crystalline epoxy composites.

EXPERIMENTAL

Materials

BPDGE was synthesized according to procedures reported in literature.[29] The chemical structure of the product was identified using Fourier transform infrared, ^{1}H-NMR. The epoxy equivalent of the product was 172 (theoretical, 149). 2,6-xylenol was supplied by ShanXi Rui Cheng Fusite Chemical, Ltd. Tetrabutyl ammonium bromide and triphenylphosphine (TPP) were catalysts purchased from Shanghai Chemical Reagent, Ltd. All other reagents were of analytical grade and used as received. Two epoxides and PN were used.

Epoxy monomer and hardener synthesis

3,3′,5,5′-tetramethyl-4,4′-biphenyl

The TMBP was synthesized using oxidative coupling reaction according to a patent[35] with modification. Into a 500 mL, four-necked flask, fitted with a additional gas tube, a condenser, a thermometer, and a stirrer capable of operating at 1000 rpm, there were added 30.5 g (250 mmol) of 2,6-xylenol, 0.15 g (0.521 mmol) of sodium laurylsulfate, 6.5 g (17.044 mmol) borax, and 250 mL of ion exchanged water. The mixture was stirred under oxygen and heated to a temperature of 55°C till the solid 2,6-xylenol was melted completely. Then the reaction mixture was heated to a temperature of 80°C while stirring at about 1000 rpm. At that time 5 mL (0.001 mmol/L) of cupric acetate solution was added, and a slow stream of oxygen was introduced. At the end of 6 h, the reaction was flushed with nitrogen and cooled to room temperature. Then 6 mL of a 3N HCl aqueous solution was added thereto to acidify. The reaction mixture was filtered under slight vacuum. The recovered solid was washed with water and dried. The unreacted 2,6-xylenol and polyphenoxy ether were removed by washing it twice with benzene and then filtrating under reduced pressure. The yellow solid powders obtained gave a melt point of 223–225°C. Yield was 67%. IR(KBr):3397 (O—H, st), 1573 (aromatic C=C, st), 1286 (aliphatic —H, st), 1286 (aromatic CH$_3$, band), 1197 (C—O(H), st); ^{1}H-NMR (CDCl$_3$, in ppm): 3.75– 5.25 (s, 2H, —OH), 2.27 (s, 12H, aromatic (—OH) —H), 7.13 (s, 4H, aromatic —H).

Diglycidyl ether of 3,3′,5,5′-tetramethyl-4,4′-biphenyl

The TMBPDGE was prepared by refluxing 10.9 g (44.986 mmol) of TMBP with excess epichlorohydrin (65 g, 702.475 mmol) in the presence of tetrabutylammonium bromide (0.48 g, 1.489 mmol) and 15 mL of isopropyl alcohol, under an atmosphere of nitrogen till the solution was clear. Then a 20 g of 30% NaOH aqueous solution was added into the mixture dropwise. At the same time, the excess epichlorohydrin and water were evaporated at 85°C under reduced pressure. Then the reaction was finished after 1 h later. The solid product was washed with water twice and was purified by recrystallization using a mixture constituted from acetone/methanol (1:2/volume). Yield was 87%. The chemical structure of the product was identified as TMBPDGE using Fourier Transform Infrared, ^{1}HNMR. IR(KBr pellet, cm^{-1}): 910 (epoxy C—O, st), 1380 (aromatic CH$_3$, band), 1201 (C—O, st), 1575 (aromatic C=C, st), 2923 (aliphatic C—H, st). ^{1}H-NMR (CDCl$_3$, in ppm): 7.15–7.17 (d, 2H, aromatic), 2.32–2.34 (d, 12H, CH$_3$), 4.03–4.06, 3.74–3.78 (dd, 4H, CH$_2$, glycidyl), 3.34–3.38 (m, 2H, CH, epoxy), 2.87– 2.87, 2.70–2.72 (tdd, 4H, CH$_2$, epoxy). The epoxy equivalent of the product was determined by the HCl/acetone titration[36] to be 198 (theoretical, 177).

Phenol novolac

A mixture comprising 15.0 g of phenol, 9.5 g of an aqueous formaldehyde solution (37–40%). 0.3 g oxalic acid and 35 mL of water was refluxed for 6 h. The water and the oxalic acid were evaporated at 100°C under reduced pressure (20–40 mmHg). Then, the unreacted phenol was removed by washing it with toluene and distillation at 160°C under reduced pressure (1–3 mmHg) for 3 h. The molecule weight of the PN was measured by Gel permeation chromatography (GPC) ($M_n = 315$ g/mol^{-1}).

Preparation of samples

Pure TMBPDGE, and composites of various concentrations of BPDGE were firstly heated above their melt points. Stoichiometric amounts of hardener were then added. The mixture was stirred to homogenous.

Sample	Heat above T_m (°C)	Precure (°C/h)	Postcure (°C/h)	Phase at end of cure
BPDGE/PN	165	100/16 + 125/16 + 145/12 + 180/5	230/1	Nematic
BPDGE/PN	165	180/6	230/1	Isotropic
TMBPDGE/PN	108	120/5 + 165/4 + 180/5	220/2	Isotropic
Composites/PN	165	100/16 + 120/5 + 145/6 + 180/5	230/1	–

Then 1 phr TPP was added as a catalyst. The liquid prepolymers were then quickly transferred to pre-warmed molds in a vented oven at the appropriate base cure temperatures. Table I shows the step-cure schedule of different epoxy resin system. The functional groups of the product were checked by FT-IR measurement and followed during curing. The peak at 912 cm^{-1}, which represents the absorption related to the asymmetric stretch of epoxy ring, is removed after post cured. The cure schedule of composite/PN system is similar to nematic phase BPDGE/PN to obtain LC domain in the final networks.

Measurements

IR spectra were recorded on a RFX-65A Fourier Transform Infrared Spectrometer. ^{1}H-NMR spectra were obtained using a DRX-400 MHz Superconducting-Magnet NMR Spectrometer with CDCl$_3$ as solvent.

Gel permeation chromatography (Waters 515-410) was carried out to estimate the number-average molecular weights and polydispersities of the polymers. Standard poly(styrene) was used for calibrating the molecular weight.

The textures of the mesophases were observed with a polarizing microscope (AXIOLAB Zeiss). Wide-angle X-ray diffraction (WAXD) studies were conducted on a D/max 1200 X-ray.

Calorimetric measurements were performed using a Perkin–Elmer Diamond DSC calorimeter, under nitrogen atmosphere to measure the heat flow under nonisothermal conditions. It was conducted from 25 to 250°C at the heating rate of 10 K/min to determine the glass transition temperature T_g.

Mechanical behavior from the glassy state to the rubbery region was studied using a DMA (TA/DMA2980). The storage (E') and the loss tangent (tan $\delta = E'' /E'$) were determined on rectangular polymer samples of approximate dimensions $2 \times 10 \times 35$ mm^3 in the three-point bending mode. The measurements were carried out in the direction of the macroscopic orientation from 40 to 220°C at a heating rate of 5°C/min and a fixed frequency of 1 Hz.

Impact test was carried out with samples of size $10 \times 50 \times 4$ mm^3 with 2 mm V-shaped notch in a Zwick/Roell (B5113.300) Impact Tester.

The morphologies of the fracture surfaces after impact tests for each composition were observed using a S-520 scanning electron microscope (SEM) at 15 kV accelerating voltage. Samples for each composition were cut to 2 mm heights. Each sample was mounted on a sample holder using an electrically conductive paint as an adhesive and coated with a thin gold layer by plasma sputtering to avoid a charging effect because of nonconductivity of the polymer.

RESULTS AND DISCUSSION

Phase structure of BPDGE and composites cured with PN

Ochi et al. reported that BPDGE could form a microdomain ordered structure when cured with catechol novolak (CN) and diamines which had neighboring active hydrogens compared with PN which could not help BPDGE to form a microdomain ordered structure while curing.[28,34] They assumed that it was because of the stereostructure of active hydrogens in the phenolic curing agents, but did not provide any POM, DSC, or WAXD information. To determine the formation of LC phase in the BPDGE/PN, the BPDGE and PN were first mixed well at 160°C, then 1 phr TPP was added in the mixture and stirred for 10 s, the mixtures were quickly brought to room temperature before gelation. The POM picture of the prepolymer of BPDGE/PN/TPP showed obvious birefringence phenomenon [Fig. 1(a)]. A threaded nematic texture was finally fixed with step-cured schedule: 100°C/16 h + 125°C/16 h + 145°C/12 h + 180°C/5 h + 230°C/1 h as seen in Figure 1(b). The nematic phase was further confirmed by WAXD result, which showed a broad peak at 2θ = 20.44° as given in Figure 2.

However, if the BPDGE/PN/TPP were cured at 160°C till gelation as reported in literature,[28,34] no birefringence was observed by POM. It is well known that the formation of liquid crystalline phases was attributed to an increase in axial ratio from chain extension. The BPDGE monomer with the short biphenol mesogen reaches gelation very quickly, especially at high temperature.[37] As a result, there was no sufficient time for the LC monomer to extend the chains effectively before extensive crosslinking took place at high temperature. This also meant that
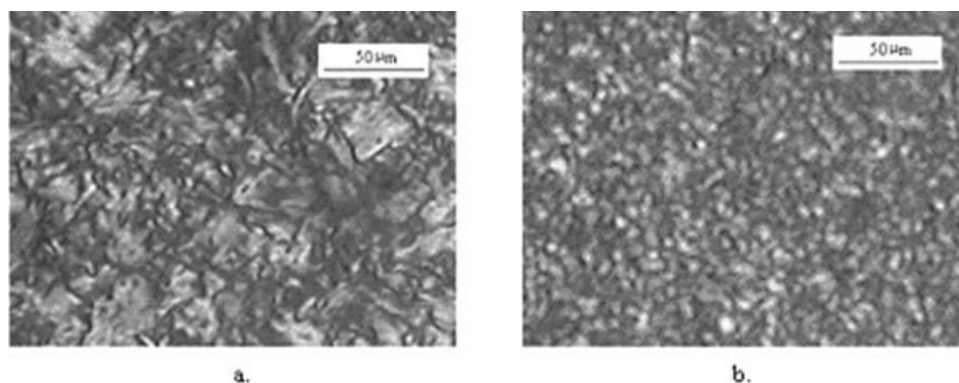
Figure 1 (a) Polarized optical microscopy of BPDGE/PN/TPP (first melted at 160 °C, then quickly brought to room temperature). (b) Polarized optical microscopy of BPDGE/PN/TPP (after post cured).

the curing schedule is the most important factor for BPDGE/PN/TPP to form a microdomain ordered structure. The BPDGE/PN/TPP only was cured at a relative low temperature the network chains can extend effectively.

Although TMBPDGE contains biphenyl mesogen, no any LC phases can be observed because of the methyl groups, which prevent the orientation of network chains. The optical morphologies of the composites were also investigated under the polarizing optical microscope. As shown in Figure 3, the bright droplet-like domains of the liquid crystalline were well dispersed in the copolymerized network and the amount of bright domains increased with the increasing BPDGE content. This suggested that LC domains could be efficiently embedded into the non LC rigid rod epoxy networks by copolymerizing with LCERs.

Dynamic mechanic analysis

Figure 4 demonstrated the dynamic mechanical properties of the thermosets employed in this study. It is
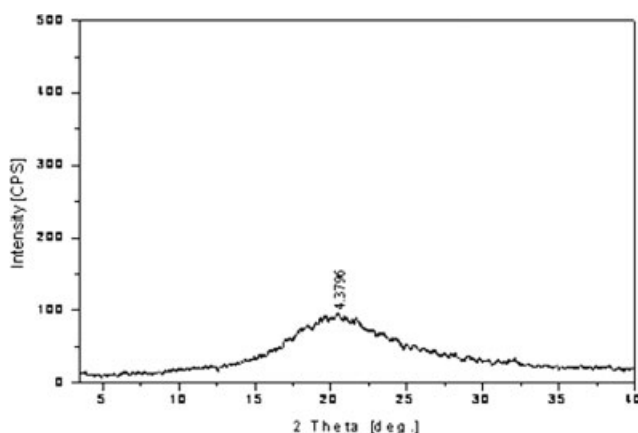

Figure 2 Wide-angle X-ray diffraction of BPDGE/BP/TPP (after postcured).

clear that tan δ goes through a maximum in the transition region and then decreases as the temperature increases. In the transition region, tan δ is high because of the initiation of micro-Brownian motion of the molecular chain segments and their stress relaxation. The cured BPDGE/TMBPDGE (50:50) composites exhibited a single relaxation peak, which indicated that there was no phase separation. We assumed that the similar reactivity of both epoxides may help the curing systems to form alternated copolymers.

It has been reported[28,34] that BPDGE/PN could not form a microdomain ordered structure during cured because the PN has no neighboring active hydrogens and the elastic modulus will decrease sharply in glass transition region if the system has no order structure. In this study, however, although the dynamic modulus (E′) of a and c rapidly decrease as the temperature of the polymer increases through T_g, the networks containing LC domain i.e., b and d display higher temperature α-relaxation and linear elastic modulus traces respectively. It is plausible to assume that when a stress is applied to an isotropic, rigid-rod network, the crosslinks are free to move in all directions without disrupting the local structure of the network. In the nematic phase, however, the crosslink motion is restricted in the direction perpendicular to the director and would result in a free energy penalty for disruption of the LC phase. In addition, in the glassy region, d displayed the lowest modulus compared to the isotropic network. It is hard to interpret these data conclusively. Since, glassy deformations are primarily governed by intermolecular van der Waals forces and short-range enthalpic deformations of the individual molecules, e.g., bending, rotating, and stretching of network strands.[38]

It can be seen from the Figure 4, the T_g of the four networks has an order: $d > c > b > a$. In this biphenol type resin system, the introduction of methyl branches must cause opposing effects on free volume which is the origin of the glass transition phenomena
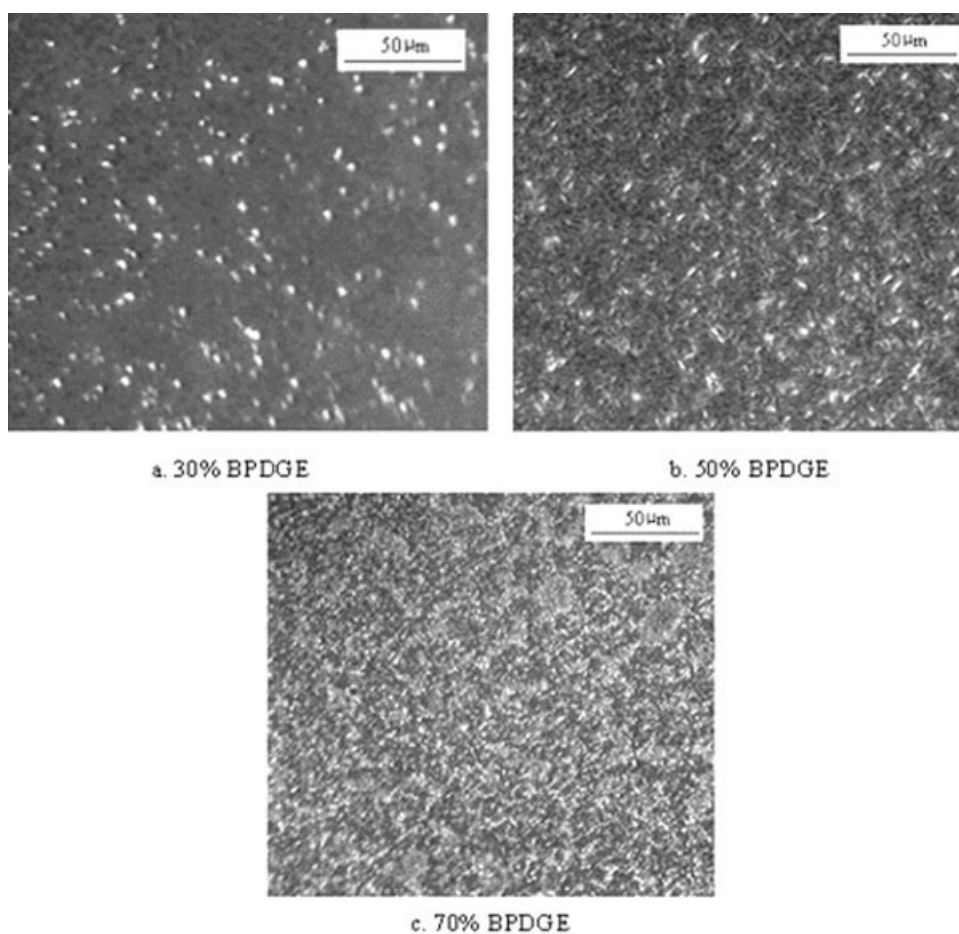
Figure 3 Polarized optical microscopy of LCER composites. (a) 30% BPDGE (b) 50% BPDGE (c) 70% BPDGE.

of polymeric materials: one effect is the increase in free volume by steric hindrance and the other effect is the decrease in free volume by filling the space between network chains. Shiraishi et al. reported that the methyl substituted groups can cause an increase in the free volume.[39] In addition, it is assumed that the molecular shapes of both phenylene groups in TMBPDGE are perpendicular because of the presence of methylic groups, which prevents the adoption of the planar structure of the biphenyl unit of BPDGE. This perpendicular structure also increases the free volume. As a result, the T_g of the cured composites decreases with the increase of methyl substituents concentration. d has a higher T_g than c due to the closer chain packing of the nematic mesophase of the LCER which decrease the free volume.

In addition, the modulus in the glassy region of TMBPDGE/PN did not decrease with the addition of BPDGE component. This may be due to the retaining of the LC domains in the composites and no obvious phase separation. This is the main advantage of LC-modified epoxy over conventional rubber—modified epoxy where a significant reduction in modulus was observed as a result of modification.[40,41]

Fracture toughness and T_g

To investigate the effect of BPDGE on the thermal and fracture toughness of the composites, impact and DSC measurements were conducted to examine the toughness and T_g. It can be seen from Figure 5 that
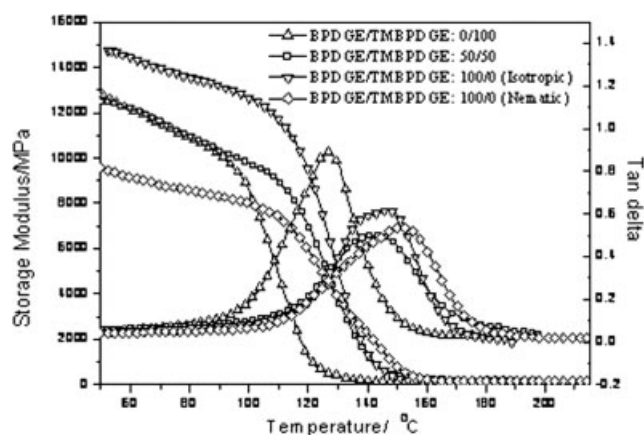
Figure 4 Loss tangent and storage modulus versus temperature plots for BPDGE/TMBPDGE composites (-Δ-) 0/100, (-○-)50/50, (-▽-) iso-100/0, and (-◇-) nem-100/0.
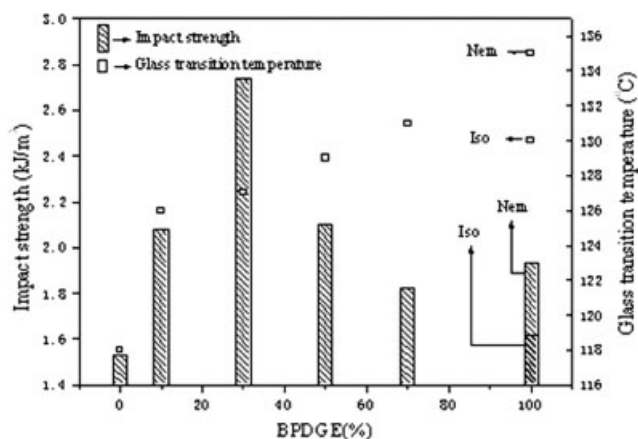
Figure 5 Comparison of impact strength and T_g for the modified curing systems (a) (nematic ×200), (b) (isotropic ×200).

the impact strength improved one- twofolds and there was a slight increase of T_g by adding BPDGE to the TMBPDGE/PN systems. This result is also seen in microscopic mechanical DMA results (Fig. 4). The inhomogeneity and the localized anisotropy may be the main reasons for the fracture toughness increase in the liquid crystalline epoxy composites. The fracture toughness improvement here is lower compared with thermoplastic modified epoxy and reactive rubber modified epoxy systems.[42] However, there is difficulty in processing this material because of different viscosities of thermoplastics and the epoxy.

Then, the *in situ* composites seem to have a θ limit, the concentration at which the LC component manifests its effect, a phenomenon as well as found in previous study[25] and also seen experimentally in thermoplastic polymer liquid crystals.[43,44] When the concentration of BPDGE increases, the modulus initially increases

and the compositions between 0 and 30% are enhanced by the effectiveness of the bridged network.
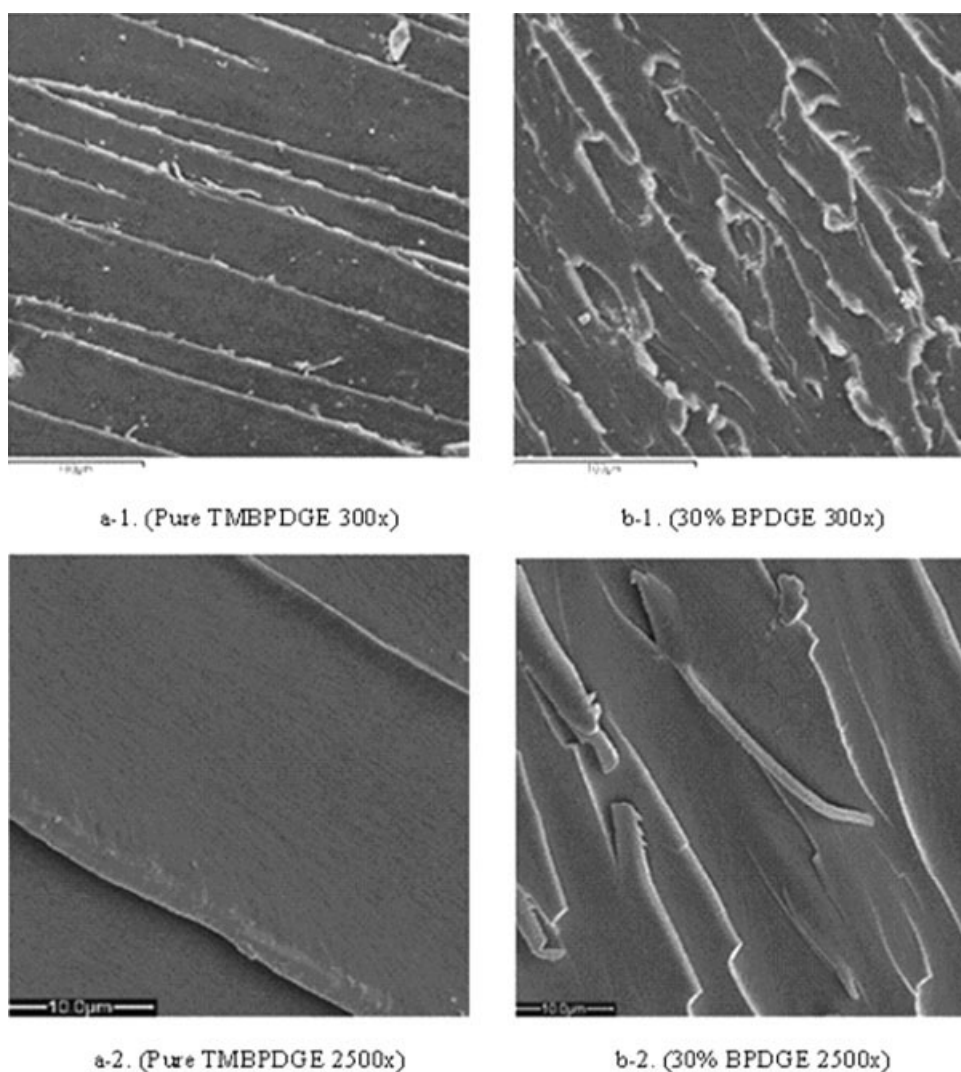
In addition, except the influence of contents of methyl substituted groups on T_g which was explained in dynamic mechanic analysis part, although a larger presence of physical crosslinks could enhance the T_g of the isotropic resin, curing in liquid crystalline state involves better reactivity of the functional groups (liquid crystalline phase facilitates the reduction of the viscosity, thus retarding gelification), enhancing the extent of the chemical crosslinks, which are clearly much more effective in increasing the T_g of the network.[45] In other words, isotropic rigid-rod TMBPDGE copolymerized with nematic BPDGE is an effective toughening method without the usual loss of T_g and modulus.

Fractography

The fracture surfaces were investigated by SEM to support the phase behaviors and mechanical results. As can be seen from Figure 6, the fracture surface of nematic BPDGE/PN [Fig. 6(a)] exhibited an extremely rough and highly deformed fracture surface, suggesting that bulk plastic deformation had occurred. The microstructure of nematic BPDGE/PN, having overall isotropic properties, consists of anisotropic domains with properties, such as strength, different along and across their molecular orientations. This leads to the deviation of crack propagation from straight line. However, the fracture surface of isotropic BPDGE/PN [Fig. 6(b)] exhibited a simple fracture surface. Low surface roughness is connected with low energy required to fracture the specimens. Miyuki et al. found that the high fracture toughness of the nematic system was because of the reorienta-

a. (nematic 200x)
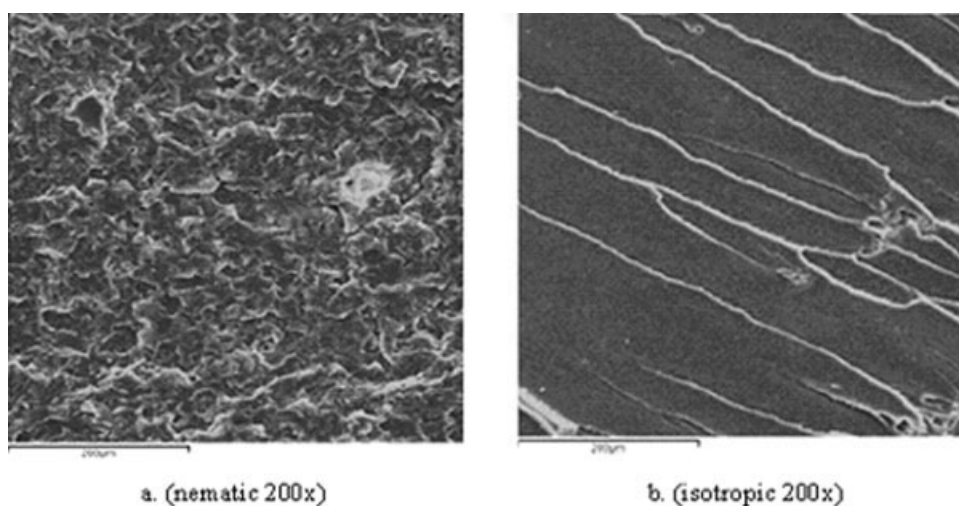
b. (isotropic 200x)

Figure 6 Fracture surface of BPDGE/PN/TPP [(a) nematic; (b) isotropic, ×200].

a-1. (Pure TMBPDGE 300x)

b-1. (30% BPDGE 300x)

a-2. (Pure TMBPDGE 2500x)

b-2. (30% BPDGE 2500x)

Figure 7 Fracture surface of TMBPDGE/PN/TPP and composites. (a-1) (Pure TMBPDGE ×300) (a-2) (Pure TMBPDGE ×2500) (b-1) (30% BPDGE ×300) (b-2) (30% BPDGE ×2500).

tion of the network chains in a wider region during the fracture process.[46]

The comparison of fractography of pure TMBPDGE and the system containing 30% BPDGE is shown in Figure 7. No obvious phase separation of the composites was observed in the high magnified image [Fig. 7 (b-2)]. This result was fairly consisted with the sole T_g of the composites measured by DMA and DSC. The fracture surfaces of the fracture specimens for modified and unmodified systems exhibit marked differences. For unmodified systems, the fracture surface is smooth, which is typical of fragile materials: the crack propagates quickly and linearly, leaving the surface homogeneous and smooth. Compared with pure TMBPDGE, the matrices containing nematic BPDGE have undergone much more plastic deformation. The presence of LC domains in the composites causes a ductile fracture. Sue et al. reported that the common fracture mechanisms of such ductile LCE

blends were crack segmentation, crack branching, crack bridging, and crack blunting.[47,48]

CONCLUSIONS

TMBPDGE based on isotropic rigid-rod epoxy was synthesized and modified by copolymerizing with BPDGE which can show LC phase after cured with PN. POM and WAXD studies indicated that with a proper step cure schedule, BPDGE will have sufficient time to form the LC domains before branching reaction takes place, which results in the formation of a nematic LC phase during the curing. The LC domains were embedded into the isotropic rigid rod epoxy networks by copolymerizing BPDGE with TMBPDGE. DMA and impact testing showed that the addition of LCER improves the toughness of pure TMBPDGE. In addition, DSC was used to investigate

the glass transition temperature of the modified systems. The results show a slight increase on T_g with the increasing of BPDGE addition. SEM also exhibited that the nematic BPDGE/PN has a rough and highly deformed fracture surface. The modified composite systems also show a quite different fracture surfaces compared with the pure TMBPDGE/PN. The orientation and/or transformation toughening may be the source for such high fracture toughness of the LCER composites.

References

1. Bagheri, R.; Pearson, R. A. J Mater Sci 1996, 31, 3945.
2. Ratna, D.; Banthia, A. K. Polym Int 2000, 49, 281.
3. Chen, T. K.; Jan, Y. H. Polym Eng Sci 1995, 35, 778.
4. Sultan, J. N.; McGarry, F. J Polym Eng Sci 1973, 13, 29.
5. Chen, J. L.; Chang, F. C. Macromolecules 1999, 32, 5348.
6. Williams, R. J. J.; Rozenberg, B. A.; Pascault, J. P. Adv Polym Sci 1997, 128, 95.
7. Galante, M. J.; Borrajo, J.; Williams, R. J. J.; Girard-Reydet, E.; Pascault, J. P. Macromolecules 2001, 34, 2686.
8. Bonnet, A.; Pascault, J. P.; Sautereau, H. Macromolecules 1999, 32, 8524.
9. Kunz, S. C.; Sayre, J. A.; Assink, R. A. Polymer 1982, 23, 1897.
10. Müller, H. P.; Gipp, R.; Heine, H.; Ger Pat. 3,622,610 (1986).
11. Dhein, R.; Müller, H. P.; Meier, H. M.; Gipp, R. Ger. Pat. 3,622,613 (1986).
12. Shiota, A.; Ober, C. K. Polymer 1997, 38, 5857.
13. Lee, J. Y.; Jang, J.; Hwang, S. S.; Hong, S. M.; Kim, K. U. Polymer 1998, 39, 6121.
14. Ochi, M.; Takashima, H. Polymer 2001, 42, 2379.
15. Mititelu1, A.; Hamaide, T.; Novat, C.; Dupuy, J.; Cascaval, C. N.; Simionescu, B. C.; Navard, P. Macromol Chem Phys 2000, 201, 1209.
16. Akatsuka, M.; Takezawa, Y. J Appl Polym Sci 2003, 89, 2464.
17. Lee, J. Y.; Shim, M. J.; Kim, S. W. J Appl Polym Sci 2002, 83, 2419.
18. Tan, C.; Sun, H.; Fung, B. M. Macromolecules 2000, 33, 6249.
19. Shiota, A.; Ober, C. K. Macromolecules 1997, 30, 4278.
20. Harada, M.; Ochi, M.; Tobita, M.; Kimura, T.; Ishigaki, T.; Shimoyama, N.; Aoki, H. J Polym Sci Part B: Polym Phys 2003, 41, 1739.
21. Brostow, W.; Faitelson, E. A.; Kamensky, M. G.; Korkhov, V. P.; Rodin, Y. P. Polymer 1999, 40, 1441.
22. Carfagna, C.; Amendola, E.; Giamberini, M. Prog Polym Sci 1997, 22, 1607.
23. Farren, C.; Akatsuka, M.; Takezawa, Y.; Itoh, Y. Polymer 2001, 42, 1507.
24. Giamberini, M.; Amendola, E.; Carfagna, C. Mol Cryst Liq Cryst 1995, 266, 9.
25. Punchaipetch, P.; Ambrogi, V.; Giamberini, M.; Brostow, W.; Carfagna, C.; D'Souza, N. A. Polymer 2002, 43, 839.
26. Sadagopan, K.; Ratna, D.; Samui, A. B. J Polym Sci Part A: Polym Chem 2003, 41, 3375.
27. Ochi, M.; Yamashita, K.; Yoshizumi, M.; Shimbo, M. J Appl Polym Sci 1989, 38, 789.
28. Ochi, M.; Shimizu, Y.; Nakanishi, Y.; Murata, Y. J Polym Sci Part B: Polym Phys 1997, 35, 397.
29. Carfagna, C.; Amendola, E.; Giamberini, M.; Filippov, A. G.; Bauer, R. S. Liq Cryst 1993, 13, 571.
30. Su, W. A. J Polym Sci Part A: Polym Chem 1993, 31, 3251.
31. Su, W. A.; Chen, K. C.; Tseng, S. Y. J Appl Polym Sci 2000, 78, 446.
32. Lu, M. G.; Shim, M. J.; Kim, S. W. Polym Eng Sci 1999, 39, 274.
33. Lu, M. G.; Shim, M. J.; Kim, S. W. Macromol Chem Phys 2001, 202, 223.
34. Ochi, M.; Tsuyuno, N.; Sakaga, K.; Nakanishi, Y.; Murata, Y. J Appl Polym Sci 1995, 56, 1161.
35. Imanari, M.; Iwane, H.; Sugawara, T. U.S. Pat. 4,564,713 (1986).
36. Bulgarian State Standard, 13342–76.
37. Gavrin, A. J.; Douglas, E. P. Macromolecules 2001, 34, 5876.
38. Ortiz, C.; Kim, R.; Rodighiero, E.; Ober, C. K.; Kramer, E. J. Macromolecules 1998, 31, 4074.
39. Shiraishi, T.; Motobe, H.; Ochi, M.; Nakanishi, Y.; Konishi, I. Polymer 1992, 33, 2975.
40. Ratna, D.; Simon, G. P. Polymer 2001, 42, 8833.
41. Ratna, D.; Chakraborty, B. C.; Deb, P. C. J Polym Mater 1997, 14, 189.
42. Martinez, I.; Martin, M. D.; Eceiza, A.; Oyanguren, P.; Mondragon, I. Polymer 2000, 41, 1027.
43. James, M. B.; Witold, B.; Michael, H.; Elizabeth, G. J. Polymer 1998, 39, 4081.
44. Witold, B.; Michael, H.; Betty, L. L. Macromolecules 1994, 27, 2262.
45. Kirchmeyer, S.; Karbach, A.; Muller, H. P.; Meier, H. M.; Dhein, R. International Conference on Crosslinked Polymers, In Proceedings of the Conference, Conference Director Prof. A. V. Patris, Luzern, Switzerland, May 30–June 1, 1990; p 167.
46. Harada, M.; Aoyama, K.; Ochi, M. J Polym Sci Part B: Polym Phys 2004, 42, 4044.
47. Sue, H. J.; Earls, J. D.; Hefner, R. E. J Mater Sci 1997, 32, 4039.
48. Sue, H. J.; Earls, J. D.; Hefner, R. E. J Mater Sci 1997, 32, 4031.